Optimization of a Multibeam Satellite-Mounted Phased Array-Fed Reflector with Power Constraints

Michael F. Palvig, Tonny Rubæk
TICRA
Copenhagen, Denmark
{mfp,tr}@ticra.com

***Abstract*—Excitation coefficients for a phased array feeding an offset reflector are optimized for use on a geostationary satellite. The design method is exemplified by optimizing beams for in-flight internet over the Atlantic at two times during a day. All sets of excitation coefficients are optimized simultaneously with power constraints to allow all beams to share 18 watt of available RF power per feed element and 1200 watt in total. The antenna operates in the Ka downlink band and is designed at 19 GHz. The reflector projected aperture diameter is 1.7 meters corresponding to 107 wavelengths. The phased feed array consists of 198 elements.**

***Index Terms*—phased array, array-fed reflector, power constraints**

I. Introduction

In the telecommunication section of the satellite market, the trend in payload design for geostationary satellites is moving from simple *bent-pipe* payloads towards so-called *smart* or *software-defined* payloads. This movement is primarily motivated by an increased demand for data services, in particular internet connectivity, and a decrease in the interest of classic television broadcast [1]–[3].

For simple broadcast services, the satellite operator will know both the location of the ground stations that will uplink the signal (typically television channels) to the satellite as well as the region to which the satellite shall broadcast. This implies that it is possible to use a relatively static configuration of the payload throughout the lifespan of the satellite and to this end, a bent-pipe configuration is very suitable.

In a *bent-pipe* configuration, the payload uses a relatively simple architecture in which a signal intended for broadcast is received by the receiving antenna in one frequency band, amplified, converted down to the frequency used for the downlink, amplified, and transmitted by the transmitting antennas. In many cases, the receiving and transmitting antenna is the same.

For data services, each user needs to have access to both an uplink and a downlink - although they do not necessarily need to have the same capacity. This implies that user beams must be provided in two different frequency bands [4], [5]. Further, in order to maximize the total user data speed, the service area is divided into multiple separate beams in which polarization and frequency diversity is applied to allow for reuse of the spectral bands: The most common scheme applied being the so-called four-color scheme [6] in which the user

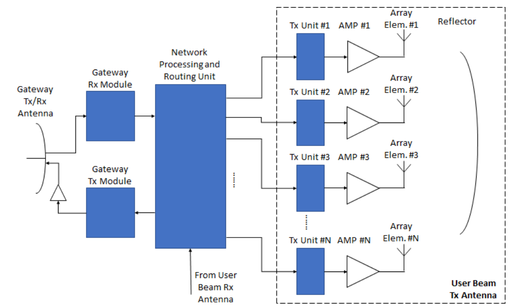

Fig. 1. Typical payload configuration for a digital payload using array-fed reflectors for the user beams. Only the Tx User Beam Antenna is included in this schematic. The User Beam Rx Antenna is assumed to be a separate array-fed reflector antenna with a set of Rx units.

beams are separated by change in polarization (left- and right-hand circular polarization) as well as frequency.

In addition, the geographical distribution of users will often change over the life-span of a mission: Either as long term changes, e.g., because roll-out of fiber internet in some rural areas decrease the demand of satellite-based internet connections. Or in short term changes, because mobile user terminals move around, e.g., with the seasonal activity of commercial fishing fleets or daily trends in global flight patterns.

This implies that it is vital for the satellite operators to be able to continuously change the shape and location of the user beams generated by the payload in order to optimize the data rate available for each user and thereby the revenue generated by the payloads [7].

A typical configuration of a software-defined payload is shown in Fig. 1. The user beams are generated by an array-fed reflector (seen on the right) and is typically using Ka or Ku band. The connection to the ground station (and the wider internet) is handled by a separate gateway antenna, operating in a different frequency band, e.g., Q or V band.

The Network Processing and Routing Unit process the data traffic, make sure each user beam has connection to the ground station, and controls the beam shapes and power levels. Data is transmitted from the unit in digital form to the Tx units of the individual array elements. These units contain digital-to-analog converters that creates IF signals containing all the beams that use the particular array element with the phase and relative amplitude required for each beam. The final step in

978-1-6654-4166-7/22/$31.00 ©2022 IEEE

the Tx units is a frequency up-converter that converts the IF signal to its final Ka band frequency. Each element then has an adjustable RF amplifier capable of amplifying the signal of the element to its final level.

Each array element can deliver a certain maximum RF power, which, because of the way the signals are generated, is to be shared by all the beams. In addition, the satellite can only support a certain amount of combined power for all the user antenna elements – and this amount of power is often lower than the power required to run all the elements at their individual maximum output power.

For maximum efficiency, it is required that user beams of both RHC and LHC polarization can be generated. This is typically done by having dual polarized feed elements with two separate inputs: One for LHC and one for RHC that combines through a suitable polarizer, e.g., a septum polarizer. In the schematic in Fig. 1, this would correspond to all even-numbered antenna elements representing LHC-polarized ports on the physical antenna elements and odd-numbered representing the RHC-polarized ports on the same elements.

The challenge in optimizing such an array-fed reflector system for a given distribution of user beams is then to optimize the phase and amplitude of the signals from each individual beam to each element in the array while at the same time respecting both the maximum output power of the individual elements as well as the total power consumption of the array.

TICRA has a long history in supplying software for array optimization to the satellite industry. In recent years, we have had a number of projects with the European Space Agency (ESA) and the major European payload manufacturers, system integrators, and satellite operators – all with the aim of improving the capabilities of the POS software product available in TICRA Tools [8] to make it meet the unique challenges posed by the design of software-defined payloads.

In this paper, we present a use case based on the recent work carried out at TICRA and illustrate how the performance of a multibeam antenna using an array-fed reflector can be optimized with respect to power consumption and EIRP requirements.

II. Use Case: In-Flight Internet in Atlantic Region

In order to illustrate the use of power constraints spanning multiple beams in an array-fed reflector we have constructed an application example. The idea behind the example is to utilize the reconfigurability of an active multibeam phased array to service the Atlantic region based on the airplane distribution at given times during the day.

Within 24 hours the distribution of flights in the Atlantic region changes drastically. The flights crossing the Atlantic follow a daily cycle: When it is evening in the US, the flights take off towards Europe. They arrive during the morning in Europe and return to the US during the day. The top images in Fig. 2 show the flight distribution at two times during a day, 12 hours apart. It is evident that the density of planes in any given geographical region is strongly varying.

To ensure that the speed of the data connections on the planes are the same for all planes, it is necessary to use different size of beams and different EIRP values in different regions of the map, depending on the density of the flights in that region. In general, the total data rate in a beam is proportional to the EIRP generated in that beam multiplied by bandwidth used in the beam. This implies that by making small beams with high EIRP in regions with a high density of flights, the data rates for the individual plane will remain as high as it is for flights in larger beams with lower EIRP.

To this end, the coverage regions in the bottom row of Fig. 2 have been defined. In these two plots, the red regions have target EIRP values of $60\,\mathrm{dB\,W}$, the green have targets of $56\,\mathrm{dB\,W}$, and the purple $52\,\mathrm{dB\,W}$. By changing the coverage regions as the day progresses, the satellite operator can provide a constant data rate to each flight – even if the density of the flights in different regions changes over the cause of the day.

III. The Antenna

The antenna is mounted on a geostationary satellite in the 40 degree west orbital slot. The antenna is configured as an array-fed reflector intended to provided user beams in the $19\,\mathrm{GHz}$ band. The reflector is paraboloid and has a projected aperture diameter of $1.7\,\mathrm{m}$ and a focal length of $3\,\mathrm{m}$. 198 dual-polarized horn antennas illuminate the reflector in a feed array. The array operates in the downlink Ka band, but for simplicity, a single frequency of $19\,\mathrm{GHz}$ is considered. The initial antenna design is synthesized in SATSOFT [9].

In Fig. 3 the the nominal beam directions, corresponding to each feed element when the array is in the focal plane of the antenna are, shown. However, to allow for an overlap between the element beams that will increase the possibilities for shaping the final composite beams of the array, the feed array has been moved 21 wavelengths closer to the reflector, thereby creating a defocused system. The $3\,\mathrm{dB}$ contour of feed element 145 is shown to illustrate the smearing effects on the element beams caused by the defocusing.

Amplification is distributed over the Tx units of the array such that each element has an amplifier capable of delivering $18\,\mathrm{W}$ of RF output power. This power must be shared among all the beams generated by the array. The satellite is able to provide a total power to the payload corresponding to $1200\,\mathrm{W}$ RF output power – well below the power required to simultaneously run all 198 feeds at their maximum output of $3564\,\mathrm{W}$ RF combined output power.

Further, it is assumed that the phase of the individual beams in each element can be set without constraints.

IV. Power-Constrained Optimization

Based on the airplane distributions in Fig. 2, a beam layout for each of the two times of the day is constructed with polygons in SATSOFT and shown in the bottom row of the figure. The beams are defined after the logic that small beams are defined where the density is high, medium sized beams

978-1-6654-4166-7/22/$31.00 ©2022 IEEE

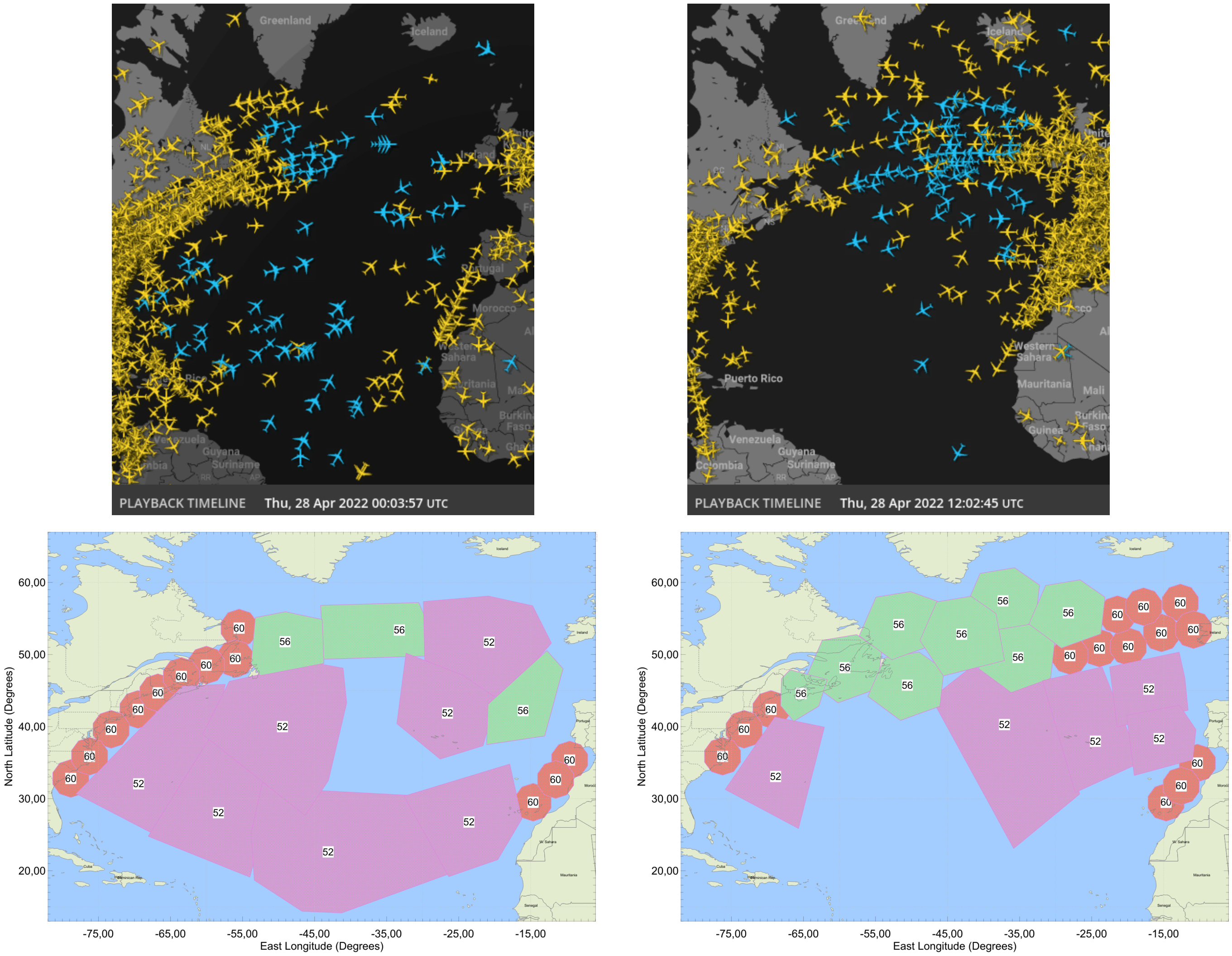

Fig. 2. Top row: Flight traffic over the Atlantic 12 hours apart (00:00UTC and 12:00UTC) on the 28th of April, 2022. Obtained from flightradar24.com. Bottom row: Coverage polygons for beams to service the 00:00UTC and 12:00UTC situations, respectively. Small beams (red) are designated an edge of coverage goal EIRP of $60\,\mathrm{dB\,W}$, medium sized beams (green) $56\,\mathrm{dB\,W}$, and large beams (purple) $52\,\mathrm{dB\,W}$.

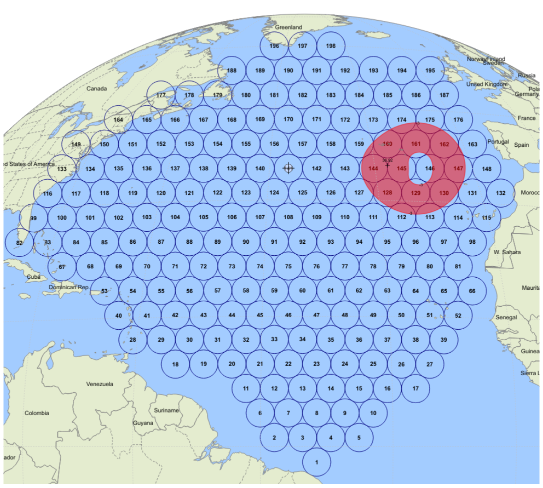

Fig. 3. Nominal beam directions corresponding to each of the 198 feeds and the defocused beam pattern of the 145th element.

where the density is moderate, and large beams where the density is low. For the 00:00UTC case, 22 coverage polygons are defined, for the 12:00UTC case 27 polygons are defined. The beam definitions are not supposed to be completely realistic, but are merely to illustrate two quite different sets of goals.

We now let SATSOFT generate a set of *synthesis stations* inside each coverage polygon. These are EIRP goals in specific far-field directions as seen from the antenna which can be understood in a POS optimization in TICRA Tools. The goal EIRP is set as follows: small beams have a goal EIRP of $60\,\mathrm{dB\,W}$, medium size beams $56\,\mathrm{dB\,W}$, and large beams $52\,\mathrm{dB\,W}$. Depending on the size of the coverage polygons, the number of synthesis stations in each polygon varies from a few tens of stations up to several hundreds.

The reflector and feed-array configuration as well as the synthesis stations are exported from SATSOFT to TICRA Tools. A multibeam array optimization is configured in POS using the Minmax algorithm such that each beam has a set of complex excitation coefficients corresponding to each element to be optimized. This corresponds to the output of the digital-to-analog converters in the Tx units, which sets the phase and the relative amplitude between the contributions to the individual beams, plus the common amplification of the RF signal at Ka band for each element.

Goals are defined for each beam and constraints are defined across all beams. The goals consist of the target minimum EIRP in each beam evaluated in the *synthesis stations*. The primary constraints are that each element may only radiate a total $18\,\mathrm{W}$ from all beams. That is, for each array element i the following constraint is imposed:

$$P_0 \sum_{j=1}^{N_{\mathrm{beams}}} |C_{ij}|^2 < 18\,\mathrm{W}, \tag{1}$$

where C_{ij} is the complex excitation coefficient for element i from beam j and P_0 is the power an element would radiate with unity excitation coefficient. With these constraints on each element, the array is allowed to radiate $198 \cdot 18\,\mathrm{W} = 3564\,\mathrm{W}$ across all elements and all beams. However, as mentioned above, the satellite can only provide power to the array corresponding to a total radiated RF power of $1200\,\mathrm{W}$. This results in an additional constraint

$$P_0 \sum_{i=1}^{N_{\mathrm{elements}}} \sum_{j=1}^{N_{\mathrm{beams}}} |C_{ij}|^2 < 1200\,\mathrm{W}. \tag{2}$$

The variables of the optimization are the real and imaginary part of the complex excitation coefficients, C_{ij}, and thus, the above constraints are nonlinear in the optimization variables.

What is evident from the constraints defined above is that the beams are interdependent: Power saved in the generation of one beam can be used for generating another beam. Therefore one cannot simply optimize the coefficients for each beam separately — coefficients for all beams must be simultaneously optimized. With 27 beams and 198 elements, 10692 variables are involved in the optimization for the 12:00UTC situation. POS employs specialized algorithms to handle this amount of optimization unknowns along with the nonlinear power constraints in an efficient way.

It is also possible to define other types of constraints as well as applying the constraints to only subsets of beams and elements instead of across all elements and beams as we have done in this example.

Other than the maximum power constraints on element and array level used for this design, it is possible to constrain minimum power and maximum dynamic range for a subset of elements. In many cases it is not possible to turn off elements completely or it may have adverse effects on the payload if it is done. Similarly, it may not be possible to have an infinite dynamic range between the signals from different beams in a single element due to the resolution in the digital-to-analog converter.

Finally, it is possible to define fixed power on both element and array level. And to define that a certain subset of elements must have the same phase, which is often the case for arrays that employ subarrays as elements.

V. Results

Two optimizations have been performed in POS, one for all the beams in the 00:00UTC case and one for all the beams in the 12:00UTC case. Both optimizations yields a solution which satisfies the required EIRP goals within the given constraints ($18\,\mathrm{W}$ per feed and $1200\,\mathrm{W}$ in total). For the 00:00UTC case the goals are fulfilled with a $1.0\,\mathrm{dB}$ margin and for the 12:00UTC case they are fulfilled with a $0.5\,\mathrm{dB}$ margin. This means that e.g. within a medium sized beam in the 12:00UTC case, the EIRP is no lower than $56.5\,\mathrm{dB}$.

The power radiated by each beam ranges between $20\,\mathrm{W}$ and $99\,\mathrm{W}$. The required power for a beam is dependent on the angular area it has to cover and the required EIRP. The constraints and goals ensure that the available feed- and total power is shared in a sensible way between the beams.

In order to visualize solution, the radiated fields from the array-fed reflector are re-imported from TICRA Tools to SATSOFT. In Fig. 4 five of the beams in each coverage scenario are plotted. The filled contour corresponding to the goal EIRP value of each beam is drawn over the coverage polygons. It is evident that the displayed beam patterns fulfill the EIRP goals that were set.

If we had optimized each beam separately, it would have been complicated to ensure that none of the distributed amplifiers would be over-saturated or that the total radiated power was kept below a certain value. And even if this was ensured by rescaling the excitation coefficients, it is highly likely that these coefficients would be suboptimal.

VI. Conclusion

In this paper a synthesis method for multibeam satellite antennas was presented. The presented method allows simultaneous optimization of all beams in a multibeam antenna such that constraints between the antennas can be imposed. This is practical for incorporating physical limitations in the design like available power of different system components which are common for all beams. Simultaneous optimization with relevant constraints can offer superior solutions compared to individual beam synthesis.

The method was exemplified with the design of a geostationary array-fed reflector antenna. It was demonstrated that the same resources of the system could be successfully reallocated to serve different coverage scenarios during a day.

References

[1] R. Swinford, B. Grau, and M. Bousquet, “High Throughput Satellites: Delivering future capacity needs,” 2015.

[2] “High Throughput on the High Seas - SES Government Solutions White Paper,” 2017.

[3] “Realizing Resilient Tactical Networks with Maximum Government Control on High-throughput Satellites - White Paper,” 2020.

[4] Y. Vasavada, R. Gopal, C. Ravishankar, G. Zakaria, and N. BenAmmar, “Architectures for next generation high throughput satellite systems,” *International Journal of Satellite Communications and Networking*, vol. 34, no. 4, pp. 523–546, Jul. 2016.

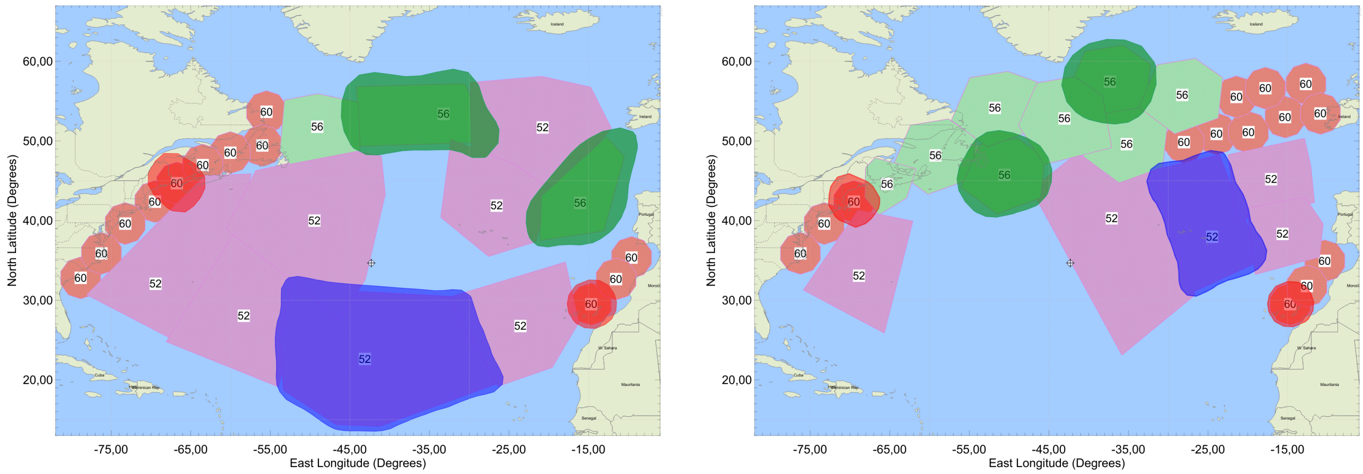

Fig. 4. The optimized radiation pattern of five of the beams in each coverage scenario plotted over the coverage polygons. The left figure is the 00:00UTC scenario and the right is the 12:00UTC scenario. Within the filled blue contours the EIRP is above $52\,\mathrm{dB\,W}$, within the green EIRP is above $56\,\mathrm{dB\,W}$, and within the red EIRP is above $60\,\mathrm{dB\,W}$.

[5] M. Takahashi, Y. Kawamoto, N. Kato, A. Miura, and M. Toyoshima, “Adaptive Power Resource Allocation With Multi-Beam Directivity Control in High-Throughput Satellite Communication Systems,” *IEEE Wireless Communications Letters*, vol. 8, no. 4, pp. 1248–1251, Aug. 2019.

[6] Teresa M. Braun and Walter R. Braun, “High-Throughput Satellites,” in *Satellite Communications Payload and System*, 2nd ed. Wiley-IEEE Press, 2021, pp. 530–549.

[7] Y. Guan, F. Geng, and J. H. Saleh, “Review of High Throughput Satellites: Market Disruptions, Affordability-Throughput Map, and the Cost Per Bit/Second Decision Tree,” *IEEE Aerospace and Electronic Systems Magazine*, vol. 34, no. 5, pp. 64–80, May 2019.

[8] TICRA, “TICRA Tools User’s Manual – TICRA Tools Version 22.0,” May 2022.

[9] ——, “SATSOFT User’s Manual - SATSOFT Version 3.5,” Dec. 2021.